TABLE 1. Summary of Experimental Data

Shot No.	Explosive System	Orientation	Pellet Thickness, mm	Arrival Times $t_1 - t_0$, μsec	Arrival Times $t_2 - t_0$, μsec	Free Surface Velocities u_{f_1}, mm/μsec	Free Surface Velocities u_{f_2}, mm/μsec	First Shock: Shock Velocity U_1, mm/μsec	First Shock: Particle Velocity u_1, mm/μsec	First Shock: Stress σ_1, kb	First Shock: V_1/V_0	First Shock: Internal Energy $E_1 - E_0$, cal/g	Second Shock: Shock Velocity U_2, mm/μsec	Second Shock: Particle Velocity u_2, mm/μsec	Second Shock: Stress σ_2, kb	Second Shock: V_2/V_0	Second Shock: Internal Energy $E_2 - E_0$, cal/g
5648	P-40 lens	X (−) to (+)	6.378	1.057	1.296	0.692	1.62	6.03	0.346	55.5	0.9426	14.3	5.05	0.810	117.0	0.8495	86.6
		X (−) to (+)	6.388	1.075	1.308	0.807	1.62	5.94	0.403	63.7	0.9320	19.5	5.03	0.810	117.4	0.8500	86.4
5807	P-40	X (+) to (−)	6.388	1.079	1.320	0.836	1.52	5.92	0.418	65.7	0.9294	20.9	4.99	0.758	110.1	0.8603	75.6
		Z	6.383	0.876		1.02		7.28	0.508	98.4	0.9302	30.9	Not observed				
5880	P-40	X (+) to (−)	6.391	1.078	1.322	0.754	(1.66)	5.93	0.377	59.4	0.9364	17.0	4.97	(0.828)	118.1	0.8444	90.5
		Initial state in Al				1.47											
5921	P-40 + 1 in. comp B	X (+) to (−)	6.380	1.079	1.146	(0.786)	2.630	5.91	0.393	(61.8)	(0.9335)	18.5	5.61	1.315	198.8	0.7686	212.0
		Y	6.347	1.020	1.144	0.994	2.56	6.22	0.497	82.2	0.9201	29.6	5.66	1.281	199.0	0.7803	206.6
5920	P-40 + 1 in. comp B	X (−) to (+)	6.391	1.069	1.139	(0.687)	2.63	5.98	0.344	(54.6)	(0.9426)	14.1	5.65	1.315	199.9	0.7702	211.7
		Z	6.380	0.876		1.40		7.28	0.698	135.1	0.9041	58.3	Not observed				
6009	P-40	Y	6.358	1.058	1.363	0.819	1.43	6.01	0.410	65.3	0.9320	20.0	4.85	0.713	103.7	0.8684	68.4
		Z	6.388	0.893		1.12		7.15	0.560	106.6	0.9215	38.2	Not observed				
5997	P-40 + 2 in. comp B	Y	6.360	1.011	1.158	1.03	3.00	6.29	0.515	86.2	0.9180	58.5	5.62	1.50	231.9	0.7411	311.9
		Z	6.386	0.871	1.201	1.40	(2.63)	7.33	0.700	136.1	0.9046	34.0	5.70	(1.32)	(227.2)	(0.7924)	217.6
7363	P-40	Z	6.599	0.914	1.824	1.04	1.58	7.22	0.520	99.8	0.9280	32.4	4.14	0.79	127.4	0.8598	102.2
		Z	3.396	0.469	0.958	1.09	1.65	7.24	0.545	104.8	0.9247	35.5	4.10	0.82	133.4	0.8519	113.6
7394	P-40 + 1 in. comp B	Z	6.607	0.899	1.336	1.27	2.32	7.35	0.635	123.6	0.9139	47.9	5.36	1.16	195.8	0.8124	193.9
		Z	3.411	0.462	0.681	1.51	2.47	7.38	0.751	147.6	0.8981	67.7	5.49	1.23	215.3	0.8066	217.2
7395	P-40	Y	6.601	1.088	1.448	0.836	1.60	6.07	0.418	67.7	0.9308	22.2	4.77	0.800	114.9	0.8495	85.3
		Y	3.399	0.562	0.745	0.862	1.58	6.05	0.431	69.3	0.9287	22.2	4.77	0.790	113.9	0.8519	85.5

Initial density, $\rho_0 = 2.6485$ g/cm³. Points in parentheses are less reliable.

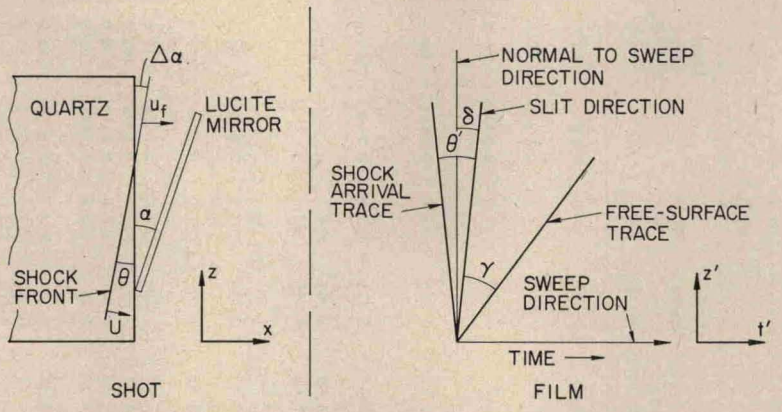

Fig. 5. Definition of parameters used in adjusting streak camera data.

error in free-surface velocity is due to uncertainty in reading the angle γ' ($\pm 1°$).

Experimental results. The observed shock velocities are plotted as functions of the shock particle velocities (taken to be one-half the free-surface velocities) in Figure 6. Data from *Wackerle* [1962] and V. Gregson (personal communication, 1963) are also shown. The data of Wackerle are his 'average" values, shown for comparison because they were determined on the same basis as the present results. The solid curves are predicted from finite strain theory. The agreement among the experimental data is seen to be generally satisfactory.

The stress-compression states were calculated from the measured velocities by means of the Rankine-Hugoniot jump conditions [*Duvall and Fowles*, 1963]:

$$V/V_0 = 1 - [(u_I - u_0)/U_I - u_0] \qquad (3)$$
$$\sigma_I - \sigma_0 = \rho_0(U_I - u_0)(u_I - u_0)$$

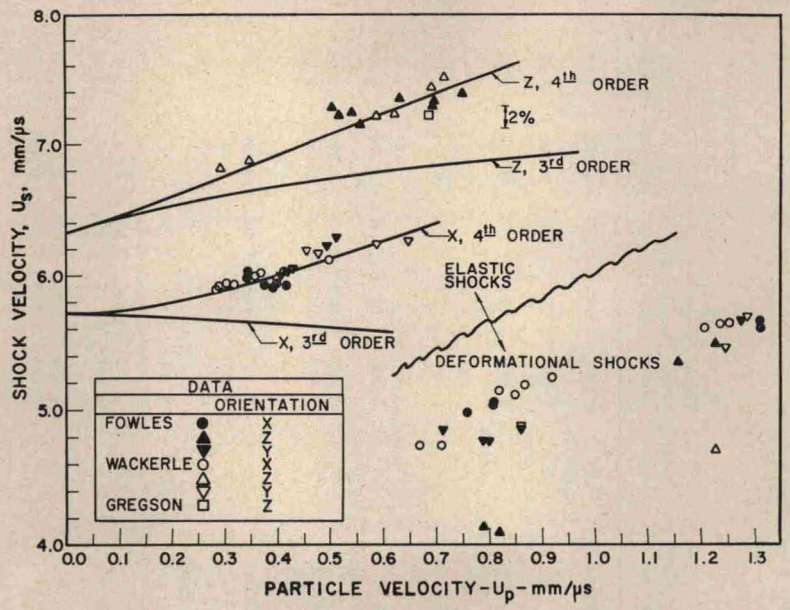

Fig. 6. Shock velocity as function of particle velocity. Curves labeled 3rd, 4th, are fits based on zero-pressure elastic constants up to third- and fourth-order, respectively, for *X*- and *Z*-cut crystals.